Published for SISSA by Springer

Received: *May 30, 2015*
Revised: *September 20, 2015*
Accepted: *September 21, 2015*
Published: *October 9, 2015*

Alternative Z' bosons in E_6

Eduardo Rojas[a,b] **and Jens Erler**[c]

[a] *Instituto de Física, Universidad de Antioquia, Calle 70 No. 52-21, Medellín, Colombia*
[b] *Laboratorio de Física Teórica e Computação Científica, Universidade Cruzeiro do Sul, 01506-000, São Paulo, Brazil*
[c] *Departamento de Física Teórica, Instituto de Física, Universidad Nacional Autónoma de México, 04510 México D.F., México*

E-mail: eduardo.rojas@cruzeirodosul.edu.br, erler@fisica.unam.mx

Abstract: We classify the quantum numbers of the extra $\mathrm{U}(1)'$ symmetries contained in E_6. In particular, we categorize the cases with rational charges and present the full list of models which arise from the chains of the maximal subgroups of E_6. As an application, the classification allows us to determine all embeddings of the Standard Model fermions in all possible decompositions of the fundamental representation of E_6 under its maximal subgroups. From this we find alternative chains of subgroups for Grand Unified Theories. We show how many of the known models including some new ones appear in alternative breaking patterns. We also use low energy constraints coming from parity-violating asymmetry measurements and atomic parity non-conservation to set limits on the E_6 motivated parameter space for a Z' boson mass of 1.2 TeV. We include projected limits for the present and upcoming QWEAK, MOLLER and SOLID experiments.

Keywords: Phenomenological Models

ArXiv ePrint: 1505.03208

Article funded by SCOAP[3].

doi:10.1007/JHEP10(2015)063

JHEP10(2015)063

Contents

1 Introduction

Heavy neutral gauge bosons are a generic prediction of many types of new physics beyond the Standard Model (SM). This is because extra $\mathrm{U}(1)'$ symmetries serve as an important model-building tool (for example, to suppress phenomenologically strongly constrained processes) giving rise — after spontaneous $\mathrm{U}(1)'$ symmetry breaking — to physical Z' vector bosons. Thus, with the advent of LHC proton-proton collisions at a center of mass energy of 13 TeV, there exists a real possibility for the on-shell production of a Z' boson [1, 2].

All representations of the E_6 gauge group [3, 4] are anomaly-free and the fundamental **27**-dimensional representation is chiral and can accommodate a full SM fermion generation. As a consequence, E_6-motivated Z' bosons arise naturally in many popular extensions of the SM [1, 5, 6], both in top-down and bottom-up constructions. Some of the E_6 subgroups, such as the original unification groups, SU(5) and SO(10), and the gauge group of left-right models, $\mathrm{SU}(4) \times \mathrm{SU}(2)_L \times \mathrm{SU}(2)_R$, play central roles in some of the best motivated extensions of the SM. Furthermore, the complete E_6-motivated Z' family of models appears in a supersymmetric bottom-up approach exploiting a set of widely accepted theoretical and phenomenological requirements [7]. The one-parameter Z' families [8], $\mathbf{10}+x\bar{\mathbf{5}}$, $d-xu$ and $q+xu$, where $\mathbf{10}$ and $\bar{\mathbf{5}}$ are SU(5) representations, q, u and d indicate U(1)$'$ quantum numbers proportional to the SM quark doublets and singlets, and x is an arbitrary real parameter, can also be discussed within the E_6 framework [9].

For all these reasons there is an expectation that an E_6 Yang-Mills theory, or a subgroup of E_6 containing the SM in a non-trivial way, might be part of a realistic theory [10]. And if a heavy vector boson is seen at the LHC or at a future even more powerful collider, aspects of the E_6 symmetry group will be central to the discussion of what this resonance might be telling us about the fundamental principles of nature.

However the discrimination between Z' models could be challenging at the LHC due to the small number of high resolution channels at hadron colliders. Another reason why the determination of the underlying symmetry structure is not straightforward is that the mass eigenstate of the Z' is in general a linear combination of some of the underlying Z' charges, with the ordinary Z boson of the SM mixed in. Hence, it is useful to reduce the theoretical possibilities or at least to have a manageable setup. This work represents an attempt in this direction and serves to spotlight a few tens of models in the two-dimensional space of E_6-motivated Z' models.

All the E_6 breaking patterns and branching rules have been tabulated in ref. [10]. The work by Robinett and Rosner [5] (hereafter referred to as RR) showed several embeddings of the SM in the decomposition $\mathbf{27} = (\mathbf{2}, \bar{\mathbf{6}}) + (\mathbf{1}, \mathbf{15})$ of the fundamental representation of E_6 under SU(2) $\times$ SU(6). Our aim here is to present an extended and more complete picture of this subject. The first goal is to find alternative chains of subgroups for Grand Unified Theories [11], which will subsequently be a useful tool towards a systematization of Z' bosons within the E_6 class.

The paper is organized as follows: in section 2 we review two different parameterizations for Z' models based on the E_6 gauge group. In section 3 we introduce a general classification of the E_6-motivated Z' models with rational charges. In section 4 we present all the E_6 chains of maximal subgroups involving U(1) symmetries and show the corresponding Z' charges and their (α, β) coordinates with respect to one of the parameterizations in section 2. Section 5 shows the exclusion limits and reach for recent and upcoming low-energy experiments for the entire E_6-motivated Z' parameter space for a Z' boson mass of $M_{Z'} = 1.2\,\mathrm{TeV}$. These low-energy measurements are competitive and highly complementary to both lepton and hadron colliders at the energy frontier.

It is important to remark that many interesting phenomenological models appear in a natural way in E_6 breaking patterns, such as the leptophobic $Z_{\not{L}}$, Z' bosons which at zero momentum transfer are proton-phobic, $Z_{\not{p}}$, or neutron-phobic, $Z_{\not{n}}$, Z' bosons from supersymmetric models, as for example the Z_N [12, 13], *etc.* Section 4 (table 4) illustrates how the best known Z' models arise naturally in this way.

2 The E_6 parameterizations

Any three linearly independent U(1) subgroups of E_6 can be used as a basis for the Z' models within this group. Once the normalization is fixed, the corresponding parameter space

JHEP10(2015)063

can be mapped to the surface of a three-dimensional sphere which can be parameterized by two angles (the rank of E_6 exceeds that of the SM by two). The α and β parameters introduced in refs. [9, 14] are the corresponding angles for the orthonormal basis Z_χ, Z_ψ and Z_Y,

$$Z' = \cos\alpha\cos\beta\, Z_\chi + \sin\alpha\cos\beta\, Z_Y + \sin\beta\, Z_\psi = \frac{c_1\, Z_R + \sqrt{3}\,(c_2\, Z_{R_1} + c_3\, Z_{L_1})}{\sqrt{c_1^2 + 3\,(c_2^2 + c_3^2)}}\ . \tag{2.1}$$

Here, the Z_Y refers to hypercharge, and the Z_χ and Z_ψ are defined through the breaking patterns $\mathrm{SO}(10) \to \mathrm{SU}(5) \times \mathrm{U}(1)_\chi$ and $E_6 \to \mathrm{SO}(10) \times \mathrm{U}(1)_\psi$, respectively. For further details and charge assignments see refs. [1, 5]. The second form appearing in eq. (2.1) uses a different orthogonal basis [9], $\mathrm{U}(1)_R$, $\mathrm{U}(1)_{R_1}$, and $\mathrm{U}(1)_{L_1}$, which are the maximal subgroups [5] defined by $\mathrm{SU}(3)_{L,R} \to \mathrm{SU}(2)_{L,R} \times \mathrm{U}(1)_{L_1,R_1}$ and $\mathrm{SU}(2)_R \to \mathrm{U}(1)_R$, referring here to the trinification subgroup [4] of $E_6 \to \mathrm{SU}(3)_C \times \mathrm{SU}(3)_L \times \mathrm{SU}(3)_R$.

In this parameterization the angles are replaced by the parameters c_1, c_2 and c_3, as indicated in eq. (2.1), together with a normalization constraint. In general the c_i are real numbers but in the most interesting cases we can usually choose them to be small integers by taking a convenient normalization. In eq. (2.1), $-\pi/2 < \beta \leq \pi/2$ is the mixing angle between the $\mathrm{U}(1)_\chi$ and $\mathrm{U}(1)_\psi$ charges, and $-\pi/2 < \alpha \leq \pi/2$ is non-vanishing when there is a mixing term [15] between hypercharge and the $\mathrm{U}(1)'$. Note, that any kinetic mixing term between the hypercharge and $\mathrm{U}(1)'$ field strength tensors can be absorbed into the value of α.

The $\mathrm{U}(1)'$ charges of the particles appearing in the fundamental representation of E_6 are shown in table 1 in terms of the parameters c_1, c_2 and c_3, satisfying

$$\tan\alpha = \frac{c_1 + c_2 + c_3}{\sqrt{\frac{2}{3}}\, c_1 - \sqrt{\frac{3}{2}}\,(c_2 + c_3)}, \qquad \tan\beta = \frac{\mathrm{sgn}[\frac{2}{3}\, c_1 - (c_2 + c_3)]}{\sqrt{\frac{2}{3}\, c_1^2 + (c_2 + c_3)^2}}(c_3 - c_2). \tag{2.2}$$

In the E_6 normalization for the hypercharge the electric charge is given by

$$Q_{em} = T_3 + \sqrt{\frac{5}{3}} Y, \tag{2.3}$$

where T_3 is the third component of weak isospin, which is $1/2$ for the neutrino. The hypercharge components in this normalization are given by eq. (2.1) with $c_1 = 3$, $c_2 = 1$ and $c_3 = 1$.

3 The E_6 structure

3.1 Decomposition of the 27 under SU(2) × SU(6)

The most important maximal subgroups of E_6 are $\mathrm{SO}(10) \times \mathrm{U}(1)$, $\mathrm{SU}(6) \times \mathrm{SU}(2)$, and $\mathrm{SU}(3) \times \mathrm{SU}(3) \times \mathrm{SU}(3)$. The representation theory of compact Lie algebras [10] implies that in the breaking $E_6 \to \mathrm{SU}(6) \times \mathrm{SU}(2)$ the fermions in the **27** are grouped into two multiplets, $\mathbf{27} \to (\mathbf{2}, \bar{\mathbf{6}}) + (\mathbf{1}, \mathbf{15})$. The multiplet $(\mathbf{2}, \bar{\mathbf{6}})$ contains six SU(2) doublets whereas fields in the $(\mathbf{1}, \mathbf{15})$ multiplet are singlets under SU(2). There are four different ways to

$l \equiv \begin{pmatrix} \nu \\ e^- \end{pmatrix}$		$-2c_2$	$-c_3$	$\bar{\nu}$	$-c_1$	$+c_2$	$+2c_3$
				e^+	$+c_1$	$+c_2$	$+2c_3$
$q \equiv \begin{pmatrix} u \\ d \end{pmatrix}$			$+c_3$	$\bar{u}$	$-c_1$	$-c_2$	
				$\bar{d}$	$+c_1$	$-c_2$	
$L \equiv \begin{pmatrix} N \\ E^- \end{pmatrix}$	$-c_1$	$+c_2$	$-c_3$	D			$-2c_3$
				$\overline{D}$		$+2c_2$	
$\overline{L} \equiv \begin{pmatrix} E^+ \\ \overline{N} \end{pmatrix}$	$+c_1$	$+c_2$	$-c_3$	S		$-2c_2$	$+2c_3$

Table 1. Charge assignment [9] for the left-handed particles and antiparticles contained in a **27**-dimensional representation of E_6 (the right-handed particles and antiparticles transforming in the antifundamental $\overline{\mathbf{27}}$ representation are implied). The upper part of the table corresponds to the **16**-dimensional representation of SO(10), while the lower part shows the **10** (with an extra anti-quark weak singlet, $\overline{D}$, of electric charge $-1/3$ and an additional weak doublet, L, as well as their SM-mirror partners) and the **1** (a SM singlet, S). This represents one fermion generation, and we assume family universality throughout. The correct normalization (*i.e.*, the one which is directly comparable to the usual normalization of the gauge couplings of $\mathrm{SU}(3)_C$ and $\mathrm{SU}(2)_L$ of the SM) of these charges is obtained upon division by $2\sqrt{c_1^2 + 3\,(c_2^2 + c_3^2)}$.

assign the SM fermions to a $\mathbf{27} = (\mathbf{2}, \overline{\mathbf{6}}) + (\mathbf{1}, \mathbf{15})$. Namely, for $E_6 \to \mathrm{SU}(2)_X \times \mathrm{SU}(6)$, where $X = L$ (left), R (right), I (inert), and A (alternative), we have

$$(\mathbf{2},\overline{\mathbf{6}})_L = \big(L, \overline{L}, q, l\big) \qquad (\mathbf{1},\mathbf{15})_L = (\overline{\nu}, S, e^+, \overline{d}, \overline{u}, D, \overline{D}) \qquad \mathrm{SU}(2)_L \tag{3.1}$$

$$(\mathbf{2},\overline{\mathbf{6}})_R = \big((\overline{d}, \overline{u}), (\overline{L}, L), (e^+, \overline{\nu})\big) \qquad (\mathbf{1},\mathbf{15})_R = (l, q, D, \overline{D}, S) \qquad \mathrm{SU}(2)_R \tag{3.2}$$

$$(\mathbf{2},\overline{\mathbf{6}})_I = \big((\overline{D}, \overline{d}), (L, l), (\overline{\nu}, S)\big) \qquad (\mathbf{1},\mathbf{15})_I = (\overline{L}, q, \overline{u}, D, e^+) \qquad \mathrm{SU}(2)_I \tag{3.3}$$

$$(\mathbf{2},\overline{\mathbf{6}})_A = \big((\overline{u}, \overline{D}), (l, \overline{L}), (S, e^+)\big) \qquad (\mathbf{1},\mathbf{15})_A = (L, q, \overline{d}, D, \overline{\nu}) \qquad \mathrm{SU}(2)_A \tag{3.4}$$

RR [5] considered the cases $X = L, R, I$. Here we add the embedding, $X = A$, to obtain a more symmetric and complete picture of the E_6 subgroups and models. The need of this embedding will become evident from the classification. One can obtain the **15** representation from the tensor product $\mathbf{6} \times \mathbf{6} = \mathbf{21}_s + \mathbf{15}_a$. Specifically, for $SU(2)_A \times \mathrm{SU}(6)$ we have explicitly (displaying only the upper-right parts of the matrix),

$$\mathbf{15} = \left[\begin{pmatrix} (\mathbf{3}_C, \mathbf{1}_L) \\ (\mathbf{1}_C, \mathbf{2}_L) \\ (\mathbf{1}_C, \mathbf{1}_L) \end{pmatrix} \times \Big((\mathbf{3}_C, \mathbf{1}_L)\ (\mathbf{1}_C, \mathbf{2}_L)\ (\mathbf{1}_C, \mathbf{1}_L) \Big)\right]_a$$

$$= \left(\begin{array}{c|c|c} (\overline{\mathbf{3}}_C, \mathbf{1}_L) & (\mathbf{3}_C, \mathbf{2}_L) & (\mathbf{3}_C, \mathbf{1}_L) \\ \hline & (\mathbf{1}_C, \mathbf{1}_L) & (\mathbf{1}_C, \mathbf{2}_L) \\ \hline & & 0 \end{array}\right) = \left(\begin{array}{ccc|cc|c} 0 & \overline{d}_3 & \overline{d}_2 & d_1 & u_1 & D_1 \\ & 0 & \overline{d}_1 & d_2 & u_2 & D_2 \\ & & 0 & d_3 & u_3 & D_3 \\ \hline & & & 0 & \overline{\nu} & E^- \\ & & & & 0 & N \\ \hline & & & & & 0 \end{array}\right). \tag{3.5}$$

The fermions in the anti-fundamental representation of SU(6) are $\overline{\mathbf{6}}_{1/2} = (\overline{u}, l, S)$ and $\overline{\mathbf{6}}_{-1/2} = \big(\overline{D}, \overline{L}, e^+\big)$, where the subscripts $\pm 1/2$ are the $\mathrm{U}(1)_A$ charges.

JHEP10(2015)063

3.2 Alternative models

We say that two Z' models have the same multiplet structure if they can be obtained from one another by swapping some fermions between the multiplets. In other words, they have equal numbers of multiplets and for every multiplet in one model there is the corresponding multiplet in the other model with the same dimension and the same charges. For example, $\mathrm{U}(1)_R$, $\mathrm{U}(1)_I$ and $\mathrm{U}(1)_A$ in table 6 of section 4 have the same multiplet structure. We refer to models with the same multiplet structure as a given Z' as alternative models of this Z'.

3.3 Generalized RR notation

To begin with, we introduce a notation for the Z' models based on the subgroups involved in specific breaking chains. This notation borrows some elements of the work by RR [5] and will be very useful to list subgroup chains:

$$\mathrm{U}(1) \equiv \begin{cases} \mathrm{U}(1)_{n-m\ m\ Z} & \text{for the U(1) in } \mathrm{SU}(n) \to \mathrm{SU}(n-m) \times \mathrm{SU}(m) \times \mathrm{U}(1) \\ \mathrm{U}(1)_{n-1\ 1\ Z} & \text{for the U(1) in } \mathrm{SU}(n) \to \mathrm{SU}(n-1) \times \mathrm{U}(1) \\ \mathrm{U}(1)_X & \text{for the U(1) in } \mathrm{SU}(2)_X \to \mathrm{U}(1) \end{cases} \tag{3.6}$$

The subscript $Z = X, XY, \overline{X}$ (the notation is introduced below) with $X, Y = R, I, A$, depends on the multiplets involved in the breaking, and in the following we will often use the abbreviation $U_{n-m\ m\ Z}$ for $\mathrm{U}(1)_{n-m\ m\ Z}$. The U_R [5] does not couple to the left-handed projection of the SM fermions, the U_I [5] corresponds to the inert model which does not couple to up-type quarks, and similarly the U_A does not couple to down-type quarks [9]. The model $U_{n-m\ m\ X}$, with subscript X, indicates that the charges are perpendicular to the $\mathrm{U}(1)_X$, *i.e.*, if $U_{n-m\ m\ X}(f)$ is the charge of fermion f under $U_{n-m\ m\ X}$, then $\sum_{\mathrm{f}\in\,\mathbf{27}} U_{n-m\ m\ X}(f) U_X(f) = 0$. For the U_X itself we have the normalization condition $\sum_{\mathrm{f}\in\,\mathbf{27}} U_X^2(f) = 3$ (the eigenvalue of the quadratic Casimir operator for the **27** in the standard normalization). We use the notation $U_{n-m\ m\ \overline{X}}$, for the alternative model of $U_{n-m\ m\ X}$ which is also perpendicular to $\mathrm{U}(1)_X$. There are two sets of models labeled with XY, the alternative models of $\mathrm{U}(1)_\chi \in \mathrm{SO}(10)$, which are referred to as $\mathrm{U}(1)_{\chi XY}$ with $X \neq Y$. These models are perpendicular to $\mathrm{U}(1)_{42X}$ and to $\mathrm{U}(1)_{32Y}$. In a similar way we define the models $\mathrm{U}(1)_{41XY}$ which are defined to be perpendicular to $U_{51\overline{X}}$ and to U_{31Y}. It is important to distinguish between the Y used for hypercharge, and $Y = R, I, A$ which appears in the generalized RR notation and in the subscripts of the charges in table 2.

A special case in RR is the model $\mathrm{U}(1)_{33}$ (RR use the alternative notation $\mathrm{U}(1)_{L1}$) motivated by the breaking $\mathrm{SU}(6) \to \mathrm{SU}(3)_C \times \mathrm{SU}(3) \times \mathrm{U}(1)_{33}$. Since a given U(1) could appear in different breaking chains, there may be several notations for a single model. *E.g.*, in the breaking $\mathrm{SU}(3)_L \to \mathrm{SU}(2)_L \times \mathrm{U}(1)_{21L}$, the group $\mathrm{U}(1)_{21L}$ corresponds to $\mathrm{U}(1)_{33}$; for that reason the alternative models of U_{33} orthogonal to U_R, U_I, U_A are $U_{21\bar{R}}$, $U_{21\bar{I}}$ and $U_{21\bar{A}}$, respectively, as is shown in table 5. Because the U_{33} is orthogonal to U_R, U_I and U_A we do not use the subscript X as in other models.

JHEP10(2015)063

	c_1	c_2	c_3
Q^l_{mnR}	l	$+n$	$+m$
Q^l_{mnI}	$-(3n+l)/2$	$-(n-l)/2$	$+m$
Q^l_{mnA}	$(3n-l)/2$	$-(n+l)/2$	$+m$

Table 2. Coefficients of the Q^l_{mnX} charges in the Z_R, Z_{R1}, Z_{L1} basis. The Q^0_{mnX} are defined as the models with integer charges perpendicular to U_X, *i.e.*, $\sum_{\mathrm{f}\in\,\mathbf{27}} Q^0_{mnX}(f)U_X(f) = 0$. Every set of Q^l_{mnX} with fixed X contains all the Z's in E_6 ($X = R, I, A$).

3.4 U(1)' classification

We will make use of the $\mathrm{SU}(2)_X$ symmetries in order to implement a classification that identifies Z' models with similar multiplet structures. For this we define Q^0_{mnX} as the models with integer charges (up to a normalization) in eq. (2.1) perpendicular to $\mathrm{U}(1)_X$, *i.e.*, $\sum_{\mathrm{f}\in\,\mathbf{27}} Q^0_{mnX}(f)U_X(f) = 0$, where m, n are integers. The explicit forms of Q^0_{nmX} are shown in table 2. The most general form for a model that is not perpendicular to U_X is the linear combination $c_1 Q^1_{00X} + Q^0_{nmX}$, with c_1 an integer different from zero and Q^1_{00X} the charges of U_X. We label it as Q^l_{mnX} and the explicit form of the charges are shown in tables 2 and 3.

In table 3 we define $Q_{mnX} \equiv Q^0_{mnX}$, and Q^{-l}_{mnX} as the conjugate of Q^l_{mnX}. For fixed X the set $\{Q^l_{mnX}\}$ (with $m, n, l \in \mathbb{Z}$) covers all E_6 Z' models, so that the $\mathrm{U}(1)'$ charges of a model can be written in different bases as Q^l_{mnX} and $Q^{l'}_{m'n'Y}$, with $X, m, n, l \neq Y, m', n', l'$. We choose as the systematic name of the model the one which minimizes $|l|$ in such a way that m, n, l are integers. For this convention the systematic name is uniquely defined in most of the cases. In cases of ambiguity, it is always possible to apply a symmetry argument to arrive at a systematic nomenclature. For example, if for a given model $|l|$ is a minimum for both $X = I$ and $X = A$ then we choose the unique name $Q^{l'}_{m'n'R}$, as is the case for the U_R, U_A and U_I models.

3.5 Alternative models in E_6

As can be seen from the middle panel in table 3, for $l \neq 0$ the alternative models of Q^l_{mnX} are Q^{-l}_{mnX} with $X = R, I, A$ and Q^l_{mnY} with $Y \neq X$. For $l = 0$, Q_{mnX} is self-conjugate, so in this case the alternative models of Q_{mnX} are Q_{nmX} with $X = R, I, A$ and Q_{nmY} with $Y \neq X$ (see the bottom panel in table 3). In the generalized RR notation if $Q_{mnX} = \mathrm{U}(1)_{m'n'X}$ then $Q_{nmX} = \mathrm{U}(1)_{m'n'\overline{X}}$. To summarize, we have

$$\text{alternative models of } Q^l_{Xmn} = \begin{cases} Q^{-l}_{Ymn} \text{ for any } Y = R, I, A & \text{if } l \neq 0 \\ Q^0_{Ymn} \text{ for any } Y \neq X & \text{if } l = 0 \\ Q^0_{Xnm} \quad n \leftrightarrow m & \text{if } l = 0 \\ -Q^l_{Xmn} & \end{cases} \tag{3.7}$$

After fixing the normalization, a global sign is still undefined. Indeed, reversing the overall sign in the charges leads, in principle, to a different model. While this sign is physical, we

JHEP10(2015)063

Q^l_{mnR}	q_m		D_{-2m}	$\overline{d}_{l-n}$	$\overline{u}_{-l-n}$	$\overline{L}_{l+n-m}$	L_{-l+n-m}	e^+_{l+n+2m}	$\overline{\nu}_{-l+n+2m}$	$\overline{D}_{2n}$	l_{-m-2n}		S_{2m-2n}
Q^l_{mnI}	q_m		D_{-2m}	$\overline{D}_{l-n}$	$\overline{d}_{-l-n}$	L_{l+n-m}	l_{-l+n-m}	$\overline{\nu}_{l+n+2m}$	$S_{-l+n+2m}$	$\overline{u}_{2n}$	$\overline{L}_{-m-2n}$		e^+_{2m-2n}
Q^l_{mnA}	q_m		D_{-2m}	$\overline{u}_{l-n}$	$\overline{D}_{-l-n}$	l_{l+n-m}	$\overline{L}_{-l+n-m}$	S_{l+n+2m}	$e^+_{-l+n+2m}$	$\overline{d}_{2n}$	L_{-m-2n}		$\overline{\nu}_{2m-2n}$
Q^{-l}_{mnR}	q_m		D_{-2m}	$\overline{u}_{l-n}$	$\overline{d}_{-l-n}$	L_{l+n-m}	$\overline{L}_{-l+n-m}$	$\overline{\nu}_{l+n+2m}$	$e^+_{-l+n+2m}$	$\overline{D}_{2n}$	l_{-m-2n}		S_{2m-2n}
Q^{-l}_{mnI}	q_m		D_{-2m}	$\overline{d}_{l-n}$	$\overline{D}_{-l-n}$	l_{l+n-m}	L_{-l+n-m}	S_{l+n+2m}	$\overline{\nu}_{-l+n+2m}$	$\overline{u}_{2n}$	$\overline{L}_{-m-2n}$		e^+_{2m-2n}
Q^{-l}_{mnA}	q_m		D_{-2m}	$\overline{D}_{l-n}$	$\overline{u}_{-l-n}$	$\overline{L}_{l+n-m}$	l_{-l+n-m}	e^+_{l+n+2m}	$S_{-l+n+2m}$	$\overline{d}_{2n}$	L_{-m-2n}		$\overline{\nu}_{2m-2n}$
$-Q^l_{nmR}$	$\overline{d}_{-l+m}$	$\overline{u}_{l+m}$	$\overline{D}_{-2m}$	q_{-n}		L_{l+n-m}	$\overline{L}_{-l+n-m}$	l_{n+2m}		D_{2n}	$e^+_{-l-m-2n}$	$\overline{\nu}_{l-m-2n}$	S_{2m-2n}
$-Q^l_{nmI}$	$\overline{D}_{-l+m}$	$\overline{d}_{l+m}$	$\overline{u}_{-2m}$	q_{-n}		l_{l+n-m}	L_{-l+n-m}	$\overline{L}_{n+2m}$		D_{2n}	$\overline{\nu}_{-l-m-2n}$	S_{l-m-2n}	e^+_{2m-2n}
$-Q^l_{nmA}$	$\overline{u}_{-l+m}$	$\overline{D}_{l+m}$	$\overline{d}_{-2m}$	q_{-n}		$\overline{L}_{l+n-m}$	l_{-l+n-m}	L_{n+2m}		D_{2n}	$S_{-l-m-2n}$	e^+_{l-m-2n}	$\overline{\nu}_{2m-2n}$

Table 3. Fermion charge assignment for the E_6-motivated Z' models. $l = 0$ corresponds to set of models with explicit $\mathrm{SU}(2)_R$, $\mathrm{SU}(2)_A$, or $\mathrm{SU}(2)_I$ symmetry, *i.e.*, $Q^0_{mnX} \perp Q^1_{00X}$. The alternative models of Q^0_{mnX} are Q^0_{nmX} with $X = R, I, A$ and Q_{nmY} with $Y \neq X$, this becomes clear by comparing the top panel against the bottom panel. Further models can be obtained from these by splitting the SU(2) doublets by adding (in general l times) the c_i of the corresponding $\pm Q^1_{X00}$. These are denoted by Q^l_{mnX}. For $l \neq 0$ the alternative models of Q^l_{mnX} are Q^{-l}_{mnY} where Y may in general be different from X. This becomes clear when one compares the top panel against the middle one.

Z'	Z_R [5]	$Z_{\not d}$ [9]	$-Z_I$ [5]	$-Z_{L_1}$ [5]	$-Z_{R_1}$ [5]	$Z_{\not p}$ [9]
RR	U_R	U_A	U_I	U_{33}	$U_{21\overline{R}}$	$U_{21\overline{A}}$
Q^l_{nm}	Q^1_{R00}	Q^1_{A00}	$-Q^1_{I00}$	Q_{X-10}	Q_{R0-1}	Q_{A01}
Z'	$-Z_{\not n}$ [9, 16]	$-Z_{B-L}$ [17]	Z_{ALR} [18]	$-Z_{\not L}$ [19]	Z_ψ [5]	Z_χ [5]
RR	$U_{21\overline{I}}$	U_{31R}	U_{31A}	U_{31I}	U_{42R}	$U_{\chi RI}$
Q^l_{mn}	Q_{I0-1}	Q_{R-1-1}	Q_{A11}	Q_{I-1-1}	Q_{R1-1}	Q^1_{A-23}
Z'	Z_N [12, 13]	Z_{χ^*}[flipped − SU(5)] [11]	Z_η [20]	Z_Y [21, 22]	Z_S [23, 24]	—
RR	$U_{\chi AI}$	$U_{\chi RA}$	U_{51I}	U_{32I}	—	—
Q^l_{mn}	$-Q^{-1}_{R-23}$	$-Q^{-1}_{I-23}$	Q_{I-2-1}	Q_{I1-2}	Q^3_{A-14}	—

Table 4. Systematic notation Q^l_{mn} and generalized RR notation for various E_6-motivated Z' bosons. All of them appear in the literature. The $Z_{\not p}$ and the $Z_{\not n}$ are bosons which do not couple — at vanishing momentum transfer and at the tree level — to protons and neutrons, respectively. Similarly, the $Z_{\not L}$, Z_I, and $Z_{\not d}$ bosons are blind, respectively, to SM leptons, up-type quarks, and down-type quarks. The Z_{B-L} couples purely vector-like while the Z_ψ has only axial-vector couplings to the ordinary fermions. For Q^l_{mn} we take the sign of the α-β parameterization eq. (2.1). For convenience the models with the same multiplet structure of the Z_χ are referred to as $U_{\chi XY}$.

can absorb it in the Z-Z' mixing angle, whose sign is then meaningful. From now on, let us just consider models of the form (2.1), *i.e.*, without a global minus in front,

$$Z' = \cos\alpha\cos\beta\, Z_\chi + \sin\alpha\cos\beta\, Z_Y + \sin\beta\, Z_\psi.$$

Since we are limiting the global sign to be positive the maximum number of models with the same structure in eq. (3.7) reduces from 12 to 6. The above analysis is summarized in eq. (3.7) and is a way to show the implications of table 3. Table 3 shows why our classification is useful and it constitutes an important summary of the present work; it is

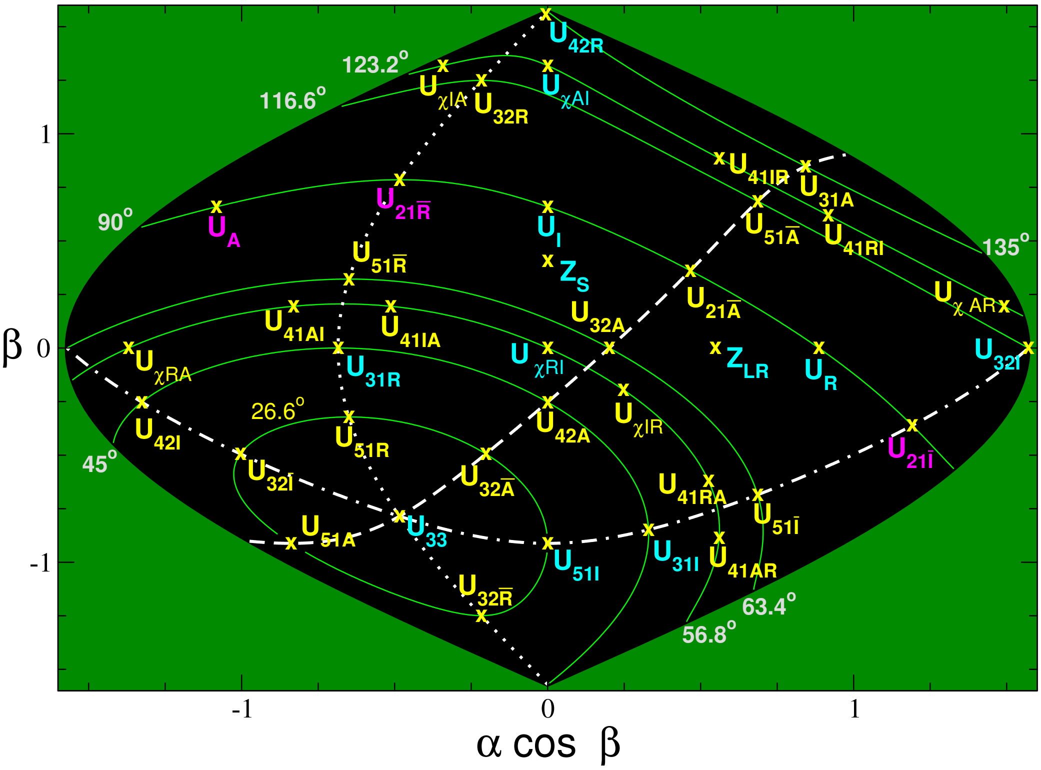

Figure 1. α-β Sanson-Flamsteed projection of E_6 Z' models. The continuous green lines correspond to all models at a fixed angle of $U_{33} = -Z_{L1}$. The white dotted, dot-dashed and dashed lines correspond to the family of models perpendicular to U_R, U_I and U_A, respectively. See the text for details. Labels in cyan correspond to very well known models in the literature (for the conventional names see table 4). Models with magenta labels are discussed in [9]; the remaining models are indicated in yellow. For every U(1) it is possible to associate a three-dimensional vector in the E_6 parameter space, the angles in degrees correspond to the angle with respect to $\mathrm{U}(1)_{33}$ as explained in section 3.6.

worth to notice that this table is valid for any Z' with rational charges in E_6. In tables 5 and 6 (see section 4) we will make use of the property $Q^{-l}_{-m-n} = -Q^{l}_{mn}$ to write the charges in a way that better reflects the underlying structure.

3.6 A geometrical interpretation

A $\mathrm{U}(1)'$ in E_6 can be written as a linear combination of an orthogonal vector basis as in eq. (2.1). We can define the dot product between two models as $\sum_{f\in \mathbf{27}} Q^{l}_{mnX}(f)\, Q^{l'}_{m'n'}(f)$. For a given Z' (for $l \neq 0$) the modulus of the cosine of the angle between the models $\pm Q^{l}_{mnX}$ and U_{33} is the same as the corresponding value between any of its alternative models and U_{33}. However there are two possible different signs for the cosine of the angle, namely $\mp\sqrt{3}m/(\sqrt{l^2+3(n^2+m^2)})$ (which are independent of X). Every sign corresponds to a curve in the α-β plane. In general, models with the same multiplet structure will appear on two different green continuous lines in figure 1. In the case $l = 0$ the modulus of the angle between models with the same multiplet structure and U_{33} could be different and, as

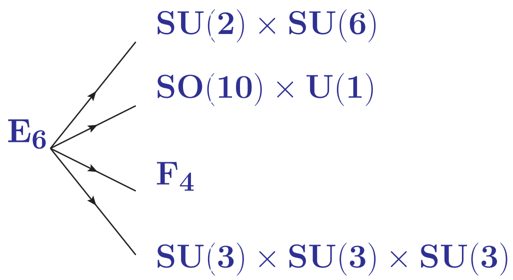

Figure 2. E_6 maximal subgroups.

in the case $l \neq 0$, the global sign of the model is also relevant. Similarly, all the alternative models of a given set of charges Q_{mnX} appear at most on two continuous green curves. All the models perpendicular to a fixed X are in a plane which contains the polar axis, which is generated by the vector U_{33}. The intersections of these planes, one for every X, with the surface of the sphere parameterized by α and β are shown in figure 1 and correspond to the models perpendicular to $\mathrm{U}(1)_R$ (dotted), $\mathrm{U}(1)_I$ (dot dashed) and $\mathrm{U}(1)_A$ (dashed). This geometrical interpretation gives us insight into the underlying structure, *i.e.,* under the present classification the models with the same multiplet structure appear in a symmetric way around the pole, which corresponds to the U_{33} model.

4 E_6 chains of subgroups

All the E_6 breaking patterns have been considered in [10] but there are different fermion assignments for the multiplets in a given breaking pattern. In the last section we studied how many different alternative models correspond to a given $\mathrm{U}(1)'$. Here we address the question whether these alternative models appear in chains of subgroups of E_6. As we will see, if a model appears in a known breaking pattern, then its alternative models will appear in the identical pattern (in most of the cases). In this way, we find the set of all possible $\mathrm{U}(1)'$ for a given breaking pattern. Once this is known, the orthogonality between the Z' is enough to determine the Z' models for every chain of maximal subgroups. In [10] the maximal subgroups of E_6 containing $U^{em}(1) \times \mathrm{SU}(3)_C$ were shown to be $\mathrm{SU}(2) \times \mathrm{SU}(6)$, $\mathrm{SO}(10) \times \mathrm{U}(1)$, F_4 and $\mathrm{SU}(3) \times \mathrm{SU}(3) \times \mathrm{SU}(3)$. We now consider the subset of those cases containing the full SM group, $\mathrm{SU}(3)_C \times \mathrm{SU}(2)_L \times \mathrm{U}(1)_Y$, instead (for a more detailed explanation see [10]).

4.1 $E_6 \to \mathrm{SU}(2)_X \times \mathrm{SU}(6)$

Considering the first case in figure 2, $\mathrm{SU}(2) \to \mathrm{SU}(2)_X$, with $X = R, I, A$, then for every chain of maximal subgroups all the U(1) factors are uniquely defined by orthogonality (see figure 3). This is because after breaking $\mathrm{SU}(2)_X$ down to $\mathrm{U}(1)_X$, all other $\mathrm{U}(1)'$ in this pattern should be perpendicular to $\mathrm{U}(1)_X$. This constraint is not present if we replace $\mathrm{SU}(2)_X$ by the unbroken SM symmetry $\mathrm{SU}(2)_L$.

JHEP10(2015)063

$\mathrm{U}(1)'$	Q^l_{mn}		c_1	c_2	c_3	$\tan\alpha$	$\tan\beta$
$\mathrm{U}(1)_R$	$+Q^1_{R00}$	$+Z_R$	1	0	0	$\sqrt{3/2}$	0
$\mathrm{U}(1)_I$	$-Q^1_{I00}$	$-Z_I$	1	-1	0	0	$\sqrt{3/5}$
$\mathrm{U}(1)_A$	$+Q^1_{A00}$	$+Z_{\not{d}}$	-1	-1	0	$-2\sqrt{6}$	$\sqrt{3/5}$
$\mathrm{U}(1)_{33}$	$+Q_{X-10}$	$-Z_{L1}$	0	0	-1	$-\sqrt{2/3}$	-1
$\mathrm{U}(1)_{21\overline{R}}$	$+Q_{R0-1}$	$-Z_{R1}$	0	-1	0	$-\sqrt{2/3}$	1
$\mathrm{U}(1)_{21\overline{I}}$	$+Q_{I0-1}$	$-Z_{\not{n}}$	$+3$	$+1$	0	$4\sqrt{2/3}$	$-1/\sqrt{7}$
$\mathrm{U}(1)_{21\overline{A}}$	$-Q_{A0-1}$	$+Z_{\not{p}}$	$+3$	-1	0	$2\sqrt{2/3}/3$	$1/\sqrt{7}$
$\mathrm{U}(1)_{31R}$	$-Q_{R11}$	$-Z_{B-L}$	0	-1	-1	$-\sqrt{2/3}$	0
$\mathrm{U}(1)_{31I}$	$-Q_{I11}$	$-Z_{\not{L}}$	3	1	-2	$2\sqrt{2/3}/3$	$-3/\sqrt{7}$
$\mathrm{U}(1)_{31A}$	$+Q_{A11}$	$+Z_{ALR}$	$+3$	-1	$+2$	$4\sqrt{2/3}$	$3/\sqrt{7}$
$\mathrm{U}(1)_{42R}$	$+Q_{R1-1}$	$+Z_\psi$	0	-1	$+1$	0	∞
$\mathrm{U}(1)_{42I}$	$-Q_{I1-1}$	—	-3	-1	-2	$-2\sqrt{6}$	$-1/\sqrt{15}$
$\mathrm{U}(1)_{42A}$	$-Q_{A1-1}$	—	$+3$	-1	-2	0	$-1/\sqrt{15}$
$\mathrm{U}(1)_{32R}$	$+Q_{R1-2}$	—	0	-2	1	$-\sqrt{2/3}$	3
$\mathrm{U}(1)_{32I}$	$+Q_{I1-2}$	$+Z_Y$	$+3$	$+1$	$+1$	∞	0
$\mathrm{U}(1)_{32A}$	$-Q_{A1-2}$	—	$+3$	-1	-1	$1/\sqrt{24}$	0
$\mathrm{U}(1)_{32\overline{R}}$	$+Q_{R-21}$	—	0	1	-2	$-\sqrt{2/3}$	-3
$\mathrm{U}(1)_{32\overline{I}}$	$+Q_{I-21}$	—	-3	-1	-4	$-8\sqrt{2/3}/3$	$-3/\sqrt{31}$
$\mathrm{U}(1)_{32\overline{A}}$	$+Q_{A-21}$	—	$+3$	-1	-4	$-2\sqrt{2/3}/7$	$-3/\sqrt{31}$
$\mathrm{U}(1)_{51R}$	$-Q_{R21}$	—	0	-1	-2	$-\sqrt{2/3}$	$-1/3$
$\mathrm{U}(1)_{51I}$	$-Q_{I21}$	$+Z_\eta$	$+3$	$+1$	-4	0	$-\sqrt{5/3}$
$\mathrm{U}(1)_{51A}$	$-Q_{A21}$	—	-3	$+1$	-4	$-2\sqrt{6}$	$-\sqrt{5/3}$
$\mathrm{U}(1)_{51\overline{R}}$	$-Q_{R12}$	—	0	-2	-1	$-\sqrt{2/3}$	$1/3$
$\mathrm{U}(1)_{51\overline{I}}$	$-Q_{I12}$	—	3	1	-1	$\sqrt{3/2}$	$-\sqrt{2/3}$
$\mathrm{U}(1)_{51\overline{A}}$	$+Q_{A12}$	—	$+3$	-1	$+1$	$\sqrt{3/2}$	$\sqrt{2/3}$
$\mathrm{U}(1)_{41IA}$	$+Q^1_{R-2-3}$	—	$+1$	-3	-2	$-4\sqrt{6}/17$	$\sqrt{3/77}$
$\mathrm{U}(1)_{41AR}$	$+Q^1_{I-2-3}$	—	2	1	-1	$\sqrt{3/2}$	$-\sqrt{3/2}$
$\mathrm{U}(1)_{41RI}$	$-Q^1_{A-2-3}$	—	5	-1	$+2$	$6\sqrt{6}/7$	$3\sqrt{3/53}$
$\mathrm{U}(1)_{41AI}$	$+Q^{-1}_{R-2-3}$	—	-1	-3	-2	$-6\sqrt{6}/13$	$\sqrt{3/77}$
$\mathrm{U}(1)_{41RA}$	$+Q^{-1}_{I-2-3}$	—	5	1	-2	$4\sqrt{6}/13$	$-3\sqrt{3/53}$
$\mathrm{U}(1)_{41IR}$	$+Q^{-1}_{A-2-3}$	—	2	-1	$+1$	$\sqrt{3/2}$	$\sqrt{3/2}$
$\mathrm{U}(1)_{\chi RI}$	$+Q^1_{A-23}$	$+Z_\chi$	2	-1	-1	0	0
$\mathrm{U}(1)_{\chi AR}$	$-Q^1_{I-23}$	—	5	1	2	$8\sqrt{6}$	$\sqrt{3/77}$
$\mathrm{U}(1)_{\chi IA}$	$-Q^1_{R-23}$	—	-1	-3	2	$-2\sqrt{6}$	$\sqrt{15}$
$\mathrm{U}(1)_{\chi IR}$	$+Q^{-1}_{A-23}$	—	5	-1	-2	$2\sqrt{6}/19$	$-\sqrt{3/77}$
$\mathrm{U}(1)_{\chi RA}$	$-Q^{-1}_{I-23}$	$+Z_{\chi*}[\mathrm{flipped}-\mathrm{SU}(5)]$	-2	-1	-1	$-2\sqrt{6}$	0
$\mathrm{U}(1)_{\chi AI}$	$-Q^{-1}_{R-23}$	$+Z_N$	1	-3	2	0	$\sqrt{15}$

Table 5. c_i and α-β coordinates for E_6-motivated Z' models appearing in E_6 breakings. We determine the $\pm$ signs in front of $Q^l_{mn} = -Q^{-l}_{-m-n}$ from the α-β parameterization in eq. (2.1) and from table 2. Models with the same multiplet structure appear in the same panel.

$\mathrm{U}(1)'$	Q^l_{mn}	Q^l_{mn}
$\mathrm{U}(1)_R$	$+Q^1_{R00}$	$(e^+,\overline{d},\overline{L})_{+1}+(l,q,D,\overline{D},S)_0+(\overline{\nu},\overline{u},L)_{-1}$
$\mathrm{U}(1)_I$	$-Q^1_{I00}$	$(\overline{\nu},\overline{D},L)_{+1}+(\overline{L},q,\overline{u},D,e^+)_0+(S,\overline{d},l)_{-1}$
$\mathrm{U}(1)_A$	$+Q^1_{A00}$	$(S,\overline{u},l)_{+1}+(L,q,\overline{d},D,\overline{\nu})_0+(e^+,\overline{D},\overline{L})_{-1}$
$\mathrm{U}(1)_{33}$	$+Q_{X-10}$	$(l,\overline{L},L)_{-1}+(\overline{u},\overline{d},\overline{D})_0+(e^+,\overline{\nu},S)_{+2}+q_{+1}+D_{-2}$
$\mathrm{U}(1)_{21\overline{R}}$	$+Q_{R0-1}$	$(e^+,\overline{\nu},\overline{L},L)_{-1}+(q,D)_0+(l,S)_{+2}+(\overline{u},\overline{d})_{+1}+\overline{D}_{-2}$
$\mathrm{U}(1)_{21\overline{I}}$	$+Q_{I0-1}$	$(S,\overline{\nu},l,L)_{-1}+(q,D)_0+(\overline{L},e^+)_{+2}+(\overline{D},\overline{d})_{+1}+\overline{u}_{-2}$
$\mathrm{U}(1)_{21\overline{A}}$	$-Q_{A0-1}$	$(S,e^+,l,\overline{L})_{-1}+(q,D)_0+(L,\overline{\nu})_{+2}+(\overline{D},\overline{u})_{+1}+\overline{d}_{-2}$
$\mathrm{U}(1)_{31R}$	$-Q_{R11}$	$(\overline{L},L,S)_0+q_{+1}+(\overline{u},\overline{d})_{-1}+(e^+,\overline{\nu})_{+3}+l_{-3}+\overline{D}_{+2}+D_{-2}$
$\mathrm{U}(1)_{31I}$	$-Q_{I11}$	$(l,L,e^+)_0+q_{+1}+(\overline{D},\overline{d})_{-1}+(S,\overline{\nu})_{+3}+\overline{L}_{-3}+\overline{u}_{+2}+D_{-2}$
$\mathrm{U}(1)_{31A}$	$+Q_{A11}$	$(l,\overline{L},\overline{\nu})_0+q_{+1}+(\overline{D},\overline{u})_{-1}+(S,e^+)_{+3}+L_{-3}+\overline{d}_{+2}+D_{-2}$
$\mathrm{U}(1)_{42R}$	$+Q_{R1-1}$	$(\overline{L},L,\overline{D},D)_{-2}+(e^+,\overline{\nu},l,q,\overline{d},\overline{u})_{+1}+S_{+4}$
$\mathrm{U}(1)_{42I}$	$-Q_{I1-1}$	$(l,L,\overline{u},D)_{-2}+(S,\overline{\nu},\overline{L},q,\overline{d},\overline{D})_{+1}+e^+_{+4}$
$\mathrm{U}(1)_{42A}$	$-Q_{A1-1}$	$(l,\overline{L},\overline{d},D)_{-2}+(S,e^+,L,q,\overline{u},\overline{D})_{+1}+\overline{\nu}_{+4}$
$\mathrm{U}(1)_{32R}$	$+Q_{R1-2}$	$(e^+,\overline{\nu})_0+q_{+1}+(\overline{u},\overline{d})_{+2}+D_{-2}+l_{+3}+(\overline{L},L)_{-3}+\overline{D}_{-4}+S_{+6}$
$\mathrm{U}(1)_{32I}$	$+Q_{I1-2}$	$(\overline{\nu},S)_0+q_{+1}+(\overline{d},\overline{D})_{+2}+D_{-2}+\overline{L}_{+3}+(l,L)_{-3}+\overline{u}_{-4}+e^+_{+6}$
$\mathrm{U}(1)_{32A}$	$-Q_{A1-2}$	$(e^+,S)_0+q_{+1}+(\overline{u},\overline{D})_{+2}+D_{-2}+L_{+3}+(l,\overline{L})_{-3}+\overline{d}_{-4}+\overline{\nu}_{+6}$
$\mathrm{U}(1)_{32\overline{R}}$	$+Q_{R-21}$	$l_0+(\overline{u},\overline{d})_{+1}+q_{+2}+\overline{D}_{-2}+(e^+,\overline{\nu})_{+3}+(\overline{L},L)_{-3}+D_{-4}+S_{+6}$
$\mathrm{U}(1)_{32\overline{I}}$	$+Q_{I-21}$	$\overline{L}_0+(\overline{d},\overline{D})_{+1}+q_{+2}+\overline{u}_{-2}+(l,L)_{-3}+(\overline{\nu},S)_{+3}+D_{-4}+e^+_{+6}$
$\mathrm{U}(1)_{32\overline{A}}$	$+Q_{A-21}$	$L_0+(\overline{u},\overline{D})_{+1}+q_{+2}+\overline{d}_{-2}+(e^+,S)_{+3}+(l,\overline{L})_{-3}+D_{-4}+\overline{\nu}_{+6}$
$\mathrm{U}(1)_{51R}$	$-Q_{R21}$	$(\overline{u},\overline{d},\overline{L},L)_{+1}+(q,\overline{D},S)_{-2}+(l,D)_{+4}+(e^+,\overline{\nu})_{-5}$
$\mathrm{U}(1)_{51I}$	$-Q_{I21}$	$(l,\overline{d},L,\overline{D})_{+1}+(q,e^+,\overline{u})_{-2}+(\overline{L},D)_{+4}+(\overline{\nu},S)_{-5}$
$\mathrm{U}(1)_{51A}$	$-Q_{A21}$	$(l,\overline{u},\overline{L},\overline{D})_{+1}+(q,\overline{\nu},\overline{d})_{-2}+(L,D)_{+4}+(e^+,S)_{-5}$
$\mathrm{U}(1)_{51\overline{R}}$	$-Q_{R12}$	$(q,\overline{L},L)_{+1}+(\overline{u},\overline{d},D,S)_{-2}+(e^+,\overline{\nu},\overline{D})_{+4}+l_{-5}$
$\mathrm{U}(1)_{51\overline{I}}$	$-Q_{I12}$	$(l,q,L)_{+1}+(e^+,\overline{d},D,\overline{D})_{-2}+(\overline{\nu},\overline{u},S)_{+4}+\overline{L}_{-5}$
$\mathrm{U}(1)_{51\overline{A}}$	$+Q_{A12}$	$(l,q,\overline{L})_{+1}+(\overline{\nu},\overline{u},D,\overline{D})_{-2}+(e^+,\overline{d},S)_{+4}+L_{-5}$
$\mathrm{U}(1)_{41IA}$	$+Q^1_{R-2-3}$	$\overline{L}_0+(L,q)_{+1}+(S,\overline{u})_{-1}+(\overline{d},D)_{-2}+(e^+,\overline{D})_{+3}+\overline{\nu}_{+4}+l_{-4}$
$\mathrm{U}(1)_{41AR}$	$+Q^1_{I-2-3}$	$L_0+(l,q)_{+1}+(e^+,\overline{d})_{-1}+(\overline{D},D)_{-2}+(\overline{\nu},\overline{u})_{+3}+S_{+4}+\overline{L}_{-4}$
$\mathrm{U}(1)_{41RI}$	$-Q^1_{A-2-3}$	$l_0+(\overline{L},q)_{+1}+(\overline{\nu},\overline{D})_{-1}+(\overline{u},D)_{-2}+(S,\overline{d})_{+3}+e^+_{+4}+L_{-4}$
$\mathrm{U}(1)_{41AI}$	$+Q^{-1}_{R-2-3}$	$L_0+(\overline{L},q)_{+1}+(S,\overline{d})_{-1}+(\overline{u},D)_{-2}+(\overline{\nu},\overline{D})_{+3}+e^+_{+4}+l_{-4}$
$\mathrm{U}(1)_{41RA}$	$+Q^{-1}_{I-2-3}$	$l_0+(L,q)_{+1}+(e^+,\overline{D})_{-1}+(\overline{d},D)_{-2}+(S,\overline{u})_{+3}+\overline{\nu}_{+4}+\overline{L}_{-4}$
$\mathrm{U}(1)_{41IR}$	$+Q^{-1}_{A-2-3}$	$\overline{L}_0+(l,q)_{+1}+(\overline{\nu},\overline{u})_{-1}+(\overline{D},D)_{-2}+(e^+,\overline{d})_{+3}+S_4+L_{-4}$
$\mathrm{U}(1)_{\chi RI}$	$+Q^1_{A-23}$	$S_0+(e^+,q,\overline{u})_{+1}+(L,\overline{D})_{+2}+(\overline{L},D)_{-2}+(l,\overline{d})_{-3}+\overline{\nu}_{+5}$
$\mathrm{U}(1)_{\chi AR}$	$-Q^1_{I-23}$	$\overline{\nu}_0+(S,q,\overline{D})_{+1}+(\overline{L},\overline{d})_{+2}+(l,D)_{-2}+(L,\overline{u})_{-3}+e^+_{+5}$
$\mathrm{U}(1)_{\chi IA}$	$-Q^1_{R-23}$	$e^+_0+(\overline{\nu},q,\overline{d})_{+1}+(l,\overline{u},)_{+2}+(L,D)_{-2}+(\overline{L},\overline{D})_{-3}+S_{+5}$
$\mathrm{U}(1)_{\chi IR}$	$+Q^{-1}_{A-23}$	$e^+_0+(S,q,\overline{D})_{+1}+(L,\overline{u})_{+2}+(l,D)_{-2}+(\overline{L},\overline{d})_{-3}+\overline{\nu}_{+5}$
$\mathrm{U}(1)_{\chi RA}$	$-Q^{-1}_{I-23}$	$S_0+(\overline{\nu},q,\overline{d})_{+1}+(\overline{L},\overline{D})_{+2}+(L,D)_{-2}+(l,\overline{u})_{-3}+e^+_{+5}$
$\mathrm{U}(1)_{\chi AI}$	$-Q^{-1}_{R-23}$	$\overline{\nu}_0+(e^+,q,\overline{u})_{+1}+(l,\overline{d})_{+2}+(\overline{L},D)_{-2}+(L,\overline{D})_{-3}+S_{+5}$

Table 6. Charge assignment for E_6-motivated Z' models (up to a normalization) appearing in E_6 breakings. We determine the $\pm$ signs in front of $Q^l_{mn}=-Q^{-l}_{-m-n}$ as in table 5. Models with the same multiplet structure appear in the same panel.

JHEP10(2015)063

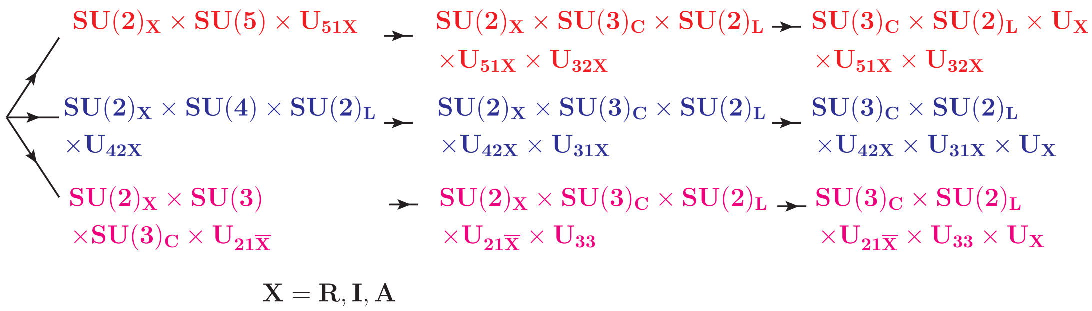

Figure 3. $E_6 \to \mathrm{SU}(2)_X \times \mathrm{SU}(6)$ chains of subgroups. All the U(1) factors are uniquely defined for a fixed X. We recall our notation $U_{n-m\ m\ Z} \equiv \mathrm{U}(1)_{n-m\ m\ Z}$. The colors are used to distinguish between the different chains of subgroups.

4.2 $\boldsymbol{E_6 \to \mathrm{SU}(2)_L \times \mathrm{SU}(6)}$

By comparing figure 3 with figure 4 corresponding to the breaking into $\mathrm{SU}(2)_X \times \mathrm{SU}(6)$ and $\mathrm{SU}(2)_L \times \mathrm{SU}(6)$, respectively, the clearest difference appears in the further breaking into $\mathrm{SU}(2)_L \times \mathrm{SU}(5) \times \mathrm{U}(1)_{51\bar{X}}$. The symmetry $\mathrm{U}(1)_{51\bar{x}}$ is an alternative model for $\mathrm{U}(1)_{51x}$ which allows two possibilities for the the SU(5) breaking, *i.e.*,

$$\mathrm{SU}(5) \to \begin{cases} \mathrm{SU}(4) \times \mathrm{U}(1)_{41XY} \\ \mathrm{SU}(3) \times \mathrm{SU}(2)_X \times \mathrm{U}(1)_{32X}. \end{cases} \tag{4.1}$$

Since $\mathrm{SU}(2)_L$ is not broken, there is just one constraint, namely the orthogonality to $\mathrm{U}(1)_{51\bar{X}}$. The models $\mathrm{U}(1)_{41XY}$ $(Y \neq X)$ are perpendicular to $\mathrm{U}(1)_{51\bar{X}}$ and $\mathrm{U}(1)_{31\bar{y}}$ (see figure 4) but they are not perpendicular to any $\mathrm{U}(1)_X$. The difference between the two SU(5) is that in one case $\mathrm{SU}(2)_L \subset \mathrm{SU}(5)$.

4.3 $\boldsymbol{E_6 \to \mathrm{U}(1) \times \mathrm{SO}(10)}$

The different fermion assignments for the breaking pattern $E_6 \to \mathrm{U}(1) \times \mathrm{SO}(10)$ are displayed in figure 5. As shown in table 4, the model Z_χ corresponds to the $\mathrm{U}(1)_{\chi RI}$ and has 5 alternative models, which are listed in table 5. Figure 5 displays the chain of subgroups, $\mathrm{U}(1)_{42X} \times \mathrm{SU}(5) \times \mathrm{U}(1)_{\chi XY} \to \mathrm{U}(1)_{42X} \times \mathrm{SU}(3)_c \times \mathrm{SU}(2)_L \times \mathrm{U}(1)_{\chi XY} \times \mathrm{U}(1)_{32Y}$, which with the choice $X = R$ and $Y = I$ results in the ordinary SU(5) unification group, with $\mathrm{U}(1)_{\chi RI}$ and $\mathrm{U}(1)_{32I}$ corresponding to the Z_χ and the hypercharge Z_Y, respectively.

The model Z_N [12, 13] is associated with $\mathrm{U}(1)_{\chi AI}$, and is an alternative model of the Z_χ appearing in the chain, $\mathrm{SO}(10) \times \mathrm{U}(1)_{42A} \to \mathrm{SU}(5) \times \mathrm{U}(1)_{42A} \times \mathrm{U}(1)_{\chi AI}$. Similarly, for every model in table 4 (except Z_S) we can find several chains of subgroups which contain them. There exist two additional chains of subgroups which we do not show in figure 5,

$$\begin{aligned} E_6 &\to \mathrm{U}(1)_{42X} \times \mathrm{SO}(10) \to \mathrm{U}(1)_{42X} \times \mathrm{SO}(9) \to \mathrm{U}(1)_{42X} \times \mathrm{SO}(7) \times \mathrm{U}(1)_X \\ &\to \mathrm{U}(1)_{42X} \times \mathrm{SU}(4) \times \mathrm{U}(1)_X \to \mathrm{U}(1)_{42X} \times \mathrm{SU}(3)_C \times \mathrm{U}(1)_X \times \mathrm{U}(1)_{31X} \end{aligned}$$

JHEP10(2015)063

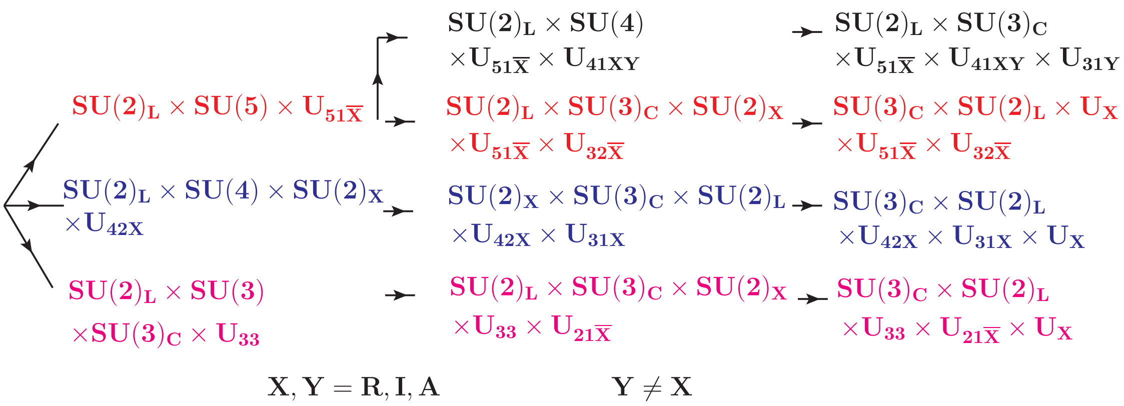

Figure 4. Same as figure 3 but for $E_6 \to \mathrm{SU}(2)_L \times \mathrm{SU}(6)$ chains of subgroups.

and the similar breaking pattern,

$$\begin{aligned} E_6 &\to \mathrm{U}(1)_{42X} \times \mathrm{SO}(10) \to \mathrm{U}(1)_{42X} \times \mathrm{SO}(9) \to \mathrm{U}(1)_{42X} \times \mathrm{SU}(4) \times \mathrm{U}(1)_X \\ &\to \mathrm{U}(1)_{42X} \times \mathrm{SU}(3)_C \times \mathrm{U}(1)_X \times \mathrm{U}(1)_{31X} \end{aligned}$$

These patterns contain $U^{em}(1) \times \mathrm{SU}(3)_C$, but not $\mathrm{SU}(2)_L$, and therefore we do not consider them as options (for further details see [10]).

4.4 $E_6 \to \mathrm{SU}(3) \times \mathrm{SU}(3) \times \mathrm{SU}(3)$

An important subgroup of E_6 for unified model building is the "trinification" group [25], which has the same rank as E_6 and the dimension of its fundamental representation is 27 as in E_6. This subgroup appears in the chain

$$\begin{aligned} E_6 &\to \mathrm{SU}(3) \times \mathrm{SU}(3) \times \mathrm{SU}(3) \to \mathrm{SU}(3)_C \times \mathrm{SU}(2)_L \times \mathrm{U}(1)_{33} \times \mathrm{SU}(3) \\ &\to \mathrm{SU}(3)_C \times \mathrm{SU}(2)_L \times \mathrm{U}(1)_{33} \times \mathrm{SU}(2)_X \times \mathrm{U}(1)_{21X} \\ &\to \mathrm{SU}(3)_C \times \mathrm{SU}(2)_L \times \mathrm{U}(1)_{33} \times \mathrm{U}(1)_X \times \mathrm{U}(1)_{21X} \end{aligned}$$

Comparison with RR shows that there are two additional models corresponding to $X = I, A$. For $X = I$ we find that the charges of the $\mathrm{U}(1)_I$ do not contribute to electric charge [6, 20]; thus, the diagonal generators of $\mathrm{SU}(3)_C \times \mathrm{SU}(2)_L \times \mathrm{U}(1)_{33} \times \mathrm{U}(1)_{21I}$ are enough to reproduce the electric charges of the fundamental representation of E_6. The same holds for $\mathrm{SU}(3)_C \times \mathrm{SU}(3)_L \times \mathrm{U}(1)_{21I}$ which provides the basis for the class of 3-3-1 models[1] [26–30].

4.5 $E_6 \to F_4 \to \mathrm{SO}(9)$

The chains of subgroups starting with $E_6 \to F_4 \to \mathrm{SO}(9)$ are similar to those containing $\mathrm{SO}(9)$ in figure 5, the unique difference being the absence of the factor $\mathrm{U}(1)_{42X}$. Due to the fact that F_4 has real or pseudo-real representations only,[2] this kind of model predicts

[1]The relationship of these models with E_6 is explored in [16].

[2]Other groups with only real or pseudo-real representations include the orthogonal groups of odd dimension, the symplectic groups, E_7 and E_8.

JHEP10(2015)063

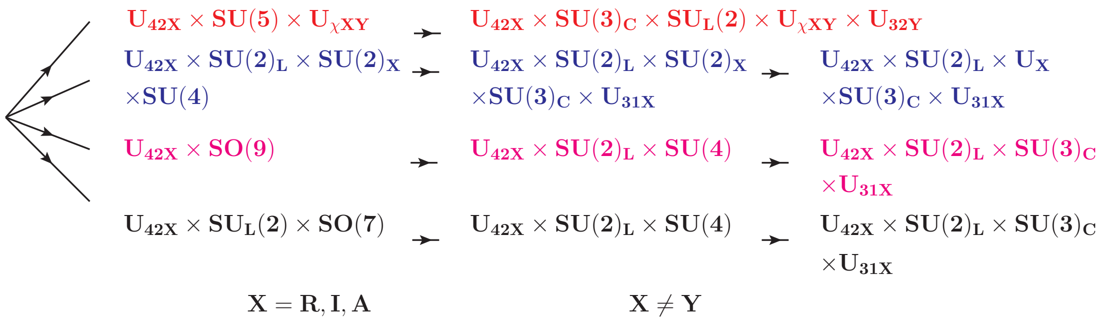

Figure 5. Same as figure 3 but for $E_6 \to \mathrm{SO}(10) \times \mathrm{U}(1)_{42X}$ chains of subgroups. One can see from table 5 that there two alternative models for the Z_ψ and five for the Z_χ.

mirror fermions which have the same quantum numbers with respect to the standard model group as the ordinary counterparts, quarks and leptons, except that they have the opposite handedness [31]. There are strong constraints on models predicting this kind of fermions [31], however they are satisfactory maximal subgroups in the sense that they contain $U_{\mathrm{em}}(1) \times \mathrm{SU}(3)_C$ (for further details and notation see [10]).

In summary, we have enumerated all the E_6 chains into maximal subgroups. The model charges and their coordinates appear in tables 5 and 6.

5 Low energy constraints on E_6

The effective parity-violating e-hadron and e-e neutral-current interactions are

$$-\mathcal{L}^{eh} = -\frac{G_f}{\sqrt{2}} \sum_i \left[C_{1i} \bar{e} \gamma_\mu \gamma^5 e \bar{q}_i \gamma^\mu q_i + C_{1i} \bar{e} \gamma_\mu e \bar{q}_i \gamma^\mu \gamma^5 q_i \right], \tag{5.1}$$

$$-\mathcal{L}^{ee} = -\frac{G_f}{\sqrt{2}} C_{2e} \bar{e} \gamma^\mu \gamma^5 e \bar{e} \gamma^\mu e. \tag{5.2}$$

Setting the Z–Z' mixing angle equal to zero [32, 33], and $\rho_1 \equiv \frac{M_W^2}{M_Z^2 \cos\theta_W} = 1$ (see [34]), then for $i = u, d$ we have

$$\begin{aligned} C_{1i} &= 2 g_A^1(e) g_V^1(i) + 2\rho_2 g'_A(e) g'_V(i), \\ C_{2i} &= 2 g_V^1(e) g_A^1(i) + 2\rho_2 g'_V(e) g'_A(i), \end{aligned} \tag{5.3}$$

where $\rho_2 \equiv (g' M_Z)^2 / (g_Z M_{Z'})^2$ and

$$g^1_{V,A}(f) = \epsilon^1_L(f) \pm \epsilon^1_R(f), \qquad g'_{V,A}(f) = \epsilon^2_L(f) \pm \epsilon^2_R(f), \tag{5.4}$$

are the corresponding vector and axial-vector couplings for the Z and Z' bosons. The quantities

$$\epsilon^1_L(f) = T_3(f) - q(f) \sin^2\theta_W^{\mathrm{eff}}, \qquad \epsilon^1_R(f) = -q(f) \sin^2\theta_W^{\mathrm{eff}}, \tag{5.5}$$

are the effective couplings of the Z boson to fermion f, where $T_3(f)$ and $q(f)$ are the third component of its weak isospin and its electric charge, respectively. The low-energy effective

JHEP10(2015)063

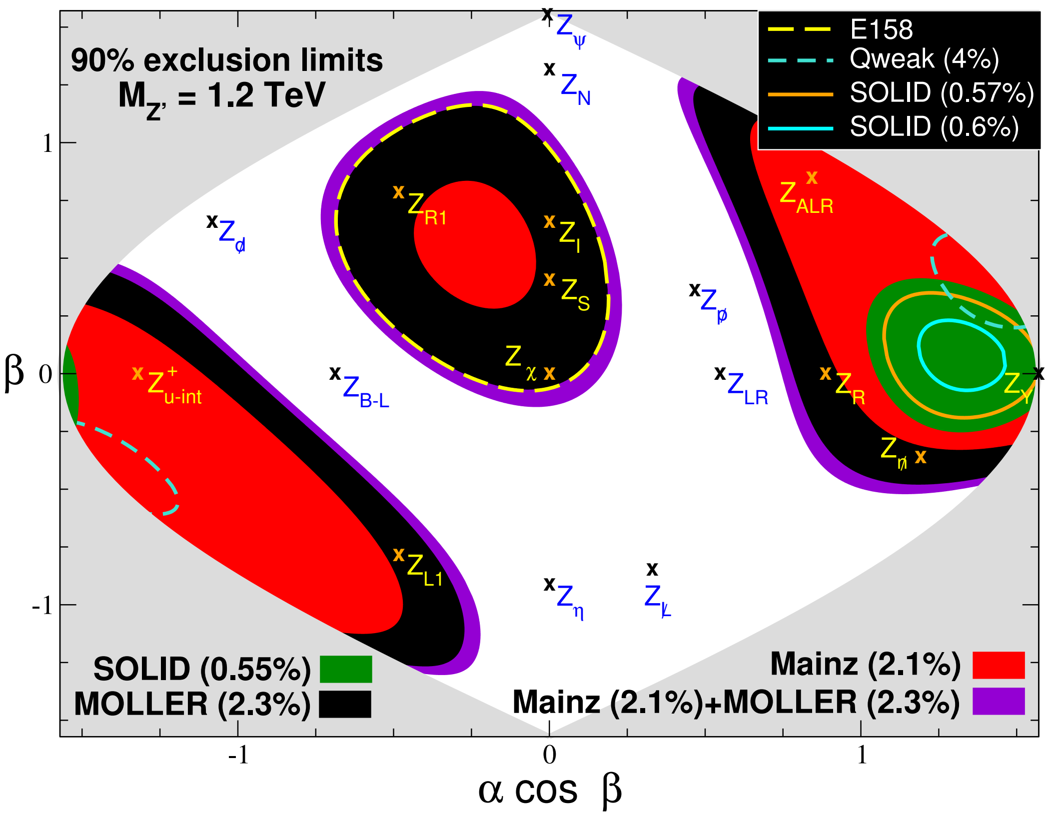

Figure 6. α-β Sanson-Flamsteed projection of E_6 Z' models. The black, red and green colored regions correspond to the 90% projected limits of the MOLLER experiment with a relative precision of 2.3%, the P2 Mainz proton weak charge measurement with a projected precision of 2.1% and the SOLID experiment at JLab assuming a measurement of parity violation in deep inelastic scattering with a relative precision of 0.55%. The yellow dashed contour encloses the 90% excluded limit by E158. The continuous orange and cyan contours enclose the 90% projected exclusion limits for a relative precision of 0.57% and 0.6% in the measurement of Q_{SOLID}. For the projected limits we assume that no deviation of the SM expectation will be found in the planned experiments.

mixing angle in the SM is $\sin^2\theta_W^{\text{eff}} = \kappa(0)\sin^2\theta_W(M_Z)_{\overline{MS}} = 0.23867$ [35, 36]. The chiral couplings for the Z' are $\epsilon_L^2(f) = Q'_L(f)$ and $\epsilon_R^2(f) = -Q'_L(\overline{f})$, where the $Q'_L(f)$ are given for some models in table 5.

The scattering of polarized (left or right-handed) electrons on an unpolarized target allows the measurement of the left-right scattering asymmetry

$$A_{\text{LR}} = \frac{d\sigma_L - d\sigma_R}{d\sigma_L + d\sigma_R}\,, \tag{5.6}$$

where $d\sigma_{L,R} \equiv d\sigma(e^-_{L,R}e^- \to e^-_{L,R}e^-)/dQ^2$ is the differential cross-section in the momentum transfer Q^2. A_{LR} differs from zero in the SM and at tree level it corresponds to a measurement of the interference between the Z boson and the photon. The A_{LR} asymmetry has been measured at low $Q^2 = 0.026\,\text{GeV}^2$ in the SLAC-E158 experiment [37], with the result

$$A_{\text{LR}} = (1.31 \pm 0.14\ (\text{stat.}) \pm 0.10\ (\text{syst.})) \times 10^{-7},$$

JHEP10(2015)063

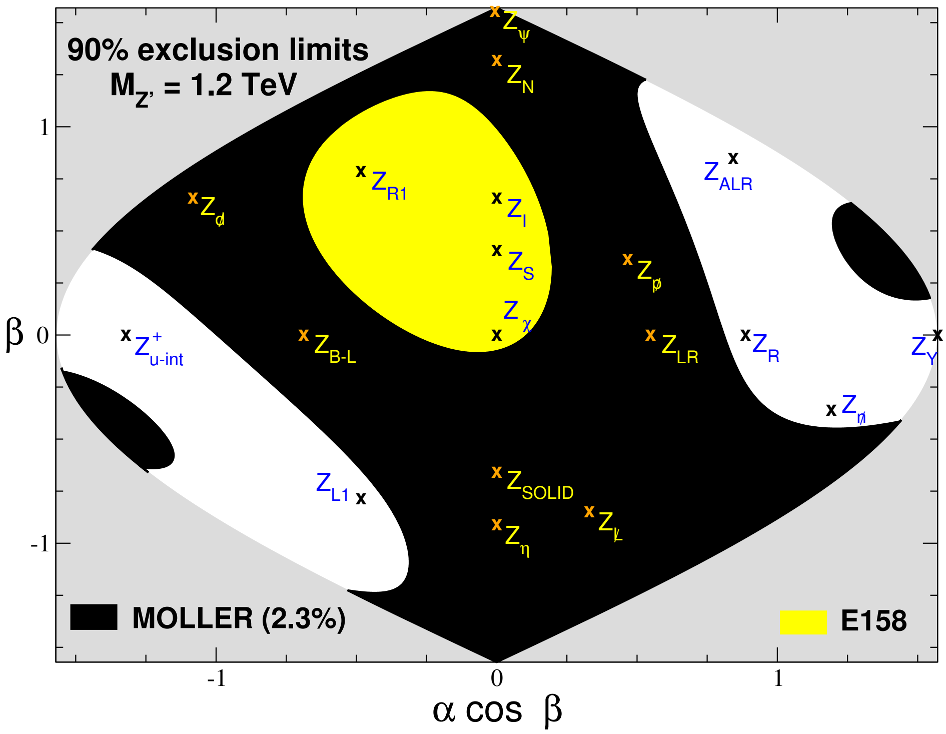

Figure 7. α-β Sanson-Flamsteed projection of E_6 Z' models. The yellow region corresponds to the 90% exclusion limit from E158. The black region corresponds to the 90% projected exclusion limit from MOLLER for a precision of 2.3%. In this case we assume a deviation in the measurement of $A_{\rm LR}$ equal to half of the deviation of E158.

leading to a determination of the weak mixing angle of $\sin^2\theta_W^{\rm eff} = 0.2403 \pm 0.0013$ [38], which is 1.25σ higher than the SM prediction [35, 36], $\sin^2\theta_W^{\rm eff} = 0.23867$. In the presence of a Z' boson the relative change of $A_{\rm LR}$ with respect to the SM expectation is given by [39, 40]

$$\frac{A_{\rm LR} - A_{\rm LR}^{\rm SM}}{A_{\rm LR}^{\rm SM}} = \frac{1}{\sqrt{2}G_F M_{Z'}^2} \frac{g'^2 g_V'(e) g_A'(e)}{1 - 4\kappa(0)\sin^2\theta_W(M_Z)_{\overline{MS}} + \cdots}, \tag{5.7}$$

where the dots stand for the one loop corrections given in [35], $A_{\rm LR}^{\rm SM}$ is the expected value of $A_{\rm LR}$ in the SM, G_F is the Fermi constant and $g' = 0.46151$ [41]. If we denote $\delta Q_W(e)$ as the change of the weak charge of the electron due to a Z' then eq. (5.7) is equal to $\delta Q_W(e)/Q_W(e)$, where $Q_W(e) = -2C_{2e}$ is the weak charge of the electron in the SM (cf. eq. (5.3)). With the upgraded electron beam at the Jefferson Laboratory (Jlab) to 12 GeV a new project called MOLLER (Measurement of Lepton-Lepton Electroweak Reaction) will improve the E158 measurement of $Q_W(e)$ by a factor of 5 [42, 43] (see figures 6 and 7). In figures 6 and 7 the $Z_{\rm SOLID} = Q^1_{R-10}$ is a boson with vector couplings to the electron and the down quark and axial coupling to the up quark. Its coordinates are $\alpha = 0$ and $\tan\beta = -\sqrt{3/5}$, and $c_1 = 1$, $c_2 = 0$, $c_3 = -1$.

The Qweak experiment at JLab [44, 45] will be able to measure the weak charge of the proton, $Q_W(p) = -2[2C_{1u} + C_{1d}]$ and $\sin^2\theta_W^{\rm eff}$ in polarized ep scattering with relative precisions of 4% and 0.3%, respectively (see figure 6). A similar experiment at the medium-energy accelerator MESA in Mainz, may be able to improve the precisions by a further factor of 2 or 2.5. A very precise determination of the weak charge of ^{12}C may also be possible [46].

The upgrade at Jlab will also allow precision measurements in parity-violating deep inelastic scattering. This project, known as SOLID (Solenoidal Large Intensity Device) [47–50], would allow 0.6% measurements of $A_{\rm LR}$ (see figure 6). One of the main goals of this experiment is the isolation of the linear combination $2C_{2u}-C_{2d}$, which is difficult to measure using elastic scattering [51, 52]. The left-right asymmetry in SOLID is proportional to $(2C_{1u}-C_{1d})+0.84(2C_{2u}-C_{2d})$.

The weak charge for an atom with N neutrons and Z protons is defined by

$$Q_W(Z,N) = -2[C_{1u}(2Z+N) + C_{1d}(Z+2N)]. \tag{5.8}$$

In the SM, $Q_W(Z,N) \approx Z(1-4\sin^2\theta_W) - N \approx -N$. There are precise experiments measuring atomic parity violation (APV) in cesium (at the 0.4% level [53]) and other heavy atoms.

These experiments (will) provide very precise determinations of the weak mixing angle off the Z peak and will be sensitive to various types of new physics [46, 48, 49, 54–56].

6 Conclusions

We have classified the two-dimensional E_6 parameter space of U(1) symmetries by means of a systematic notation. This classification allows to identify Z' models with the same multiplet structure and is convenient to determine the U(1) factors for chains of maximal subgroups of E_6 and its alternative versions. For these U(1) groups we presented the α-β coordinates and the respective charges of the fundamental representation of E_6. We also used low energy constraints from current and future parity violating asymmetry measurements and atomic parity non-conservation in order to set 90% C.L. projected limits on the entire E_6 parameter space for a reference mass of $M_{Z'} = 1.2\,\text{TeV}$.

Acknowledgments

It is a pleasure to thank Krishna Kumar for valuable suggestions regarding figures. J.E. is supported by PAPIIT (DGAPA-UNAM) project IN106913 and CONACyT (México) project 151234. E.R. acknowledges financial support provided by FAPESP, "Patrimonio Autónomo Fondo Nacional de Financiamiento para la Ciencia, la Tecnología y la Innovación, Francisco José de Caldas" and "Sostenibilidad-UDEA 2014–2015".

References

[1] P. Langacker, *The physics of heavy Z' gauge bosons*, *Rev. Mod. Phys.* **81** (2009) 1199 [arXiv:0801.1345] [INSPIRE].

[2] C. Salazar, R.H. Benavides, W.A. Ponce and E. Rojas, *LHC constraints on* 3-3-1 *models*, *JHEP* **07** (2015) 096 [arXiv:1503.03519] [INSPIRE].

[3] F. Gursey, P. Ramond and P. Sikivie, *A universal gauge theory model based on E_6*, *Phys. Lett.* **B 60** (1976) 177 [INSPIRE].

[4] Y. Achiman and B. Stech, *Quark lepton symmetry and mass scales in an E_6 unified gauge model*, *Phys. Lett.* **B 77** (1978) 389 [INSPIRE].

[5] R.W. Robinett and J.L. Rosner, *Mass scales in grand unified theories*, *Phys. Rev.* **D 26** (1982) 2396 [INSPIRE].

[6] D. London and J.L. Rosner, *Extra gauge bosons in E_6*, *Phys. Rev.* **D 34** (1986) 1530 [INSPIRE].

[7] J. Erler, *Chiral models of weak scale supersymmetry*, *Nucl. Phys.* **B 586** (2000) 73 [hep-ph/0006051] [INSPIRE].

[8] M. Carena, A. Daleo, B.A. Dobrescu and T.M.P. Tait, *Z' gauge bosons at the Tevatron*, *Phys. Rev.* **D 70** (2004) 093009 [hep-ph/0408098] [INSPIRE].

[9] J. Erler, P. Langacker, S. Munir and E. Rojas, *Z' bosons at colliders: a bayesian viewpoint*, *JHEP* **11** (2011) 076 [arXiv:1103.2659] [INSPIRE].

[10] R. Slansky, *Group theory for unified model building*, *Phys. Rept.* **79** (1981) 1 [INSPIRE].

[11] S.M. Barr, *A new symmetry breaking pattern for* SO(10) *and proton decay*, *Phys. Lett.* **B 112** (1982) 219 [INSPIRE].

[12] E. Ma, *Neutrino masses in an extended gauge model with E_6 particle content*, *Phys. Lett.* **B 380** (1996) 286 [hep-ph/9507348] [INSPIRE].

[13] S.F. King, S. Moretti and R. Nevzorov, *Theory and phenomenology of an exceptional supersymmetric standard model*, *Phys. Rev.* **D 73** (2006) 035009 [hep-ph/0510419] [INSPIRE].

[14] J. Erler and P. Langacker, *Indications for an extra neutral gauge boson in electroweak precision data*, *Phys. Rev. Lett.* **84** (2000) 212 [hep-ph/9910315] [INSPIRE].

[15] B. Holdom, *Two* U(1)*'s and epsilon charge shifts*, *Phys. Lett.* **B 166** (1986) 196 [INSPIRE].

[16] L.A. Sanchez, W.A. Ponce and R. Martinez, $\mathrm{SU}(3)(c) \times \mathrm{SU}(3)(\ell) \times \mathrm{U}(1)(X)$ *as an E_6 subgroup*, *Phys. Rev.* **D 64** (2001) 075013 [hep-ph/0103244] [INSPIRE].

[17] J.C. Pati and A. Salam, *Lepton number as the fourth color*, *Phys. Rev.* **D 10** (1974) 275 [*Erratum ibid.* **D 11** (1975) 703] [INSPIRE].

[18] E. Ma, *Particle dichotomy and left-right decomposition of E_6 superstring models*, *Phys. Rev.* **D 36** (1987) 274 [INSPIRE].

[19] K.S. Babu, C.F. Kolda and J. March-Russell, *Leptophobic* U(1)*s and the $R(b)$-$R(c)$ crisis*, *Phys. Rev.* **D 54** (1996) 4635 [hep-ph/9603212] [INSPIRE].

[20] E. Witten, *Symmetry breaking patterns in superstring models*, *Nucl. Phys.* **B 258** (1985) 75 [INSPIRE].

JHEP10(2015)063

[21] S. Glashow, *Partial symmetries of weak interactions*, Nucl. Phys. **22** (1961) 579.

[22] S. Weinberg, *A model of leptons*, Phys. Rev. Lett. **19** (1967) 1264 [INSPIRE].

[23] J. Erler, P. Langacker and T.-j. Li, *The Z-Z' mass hierarchy in a supersymmetric model with a secluded* U(1)*-prime breaking sector*, Phys. Rev. **D 66** (2002) 015002 [hep-ph/0205001] [INSPIRE].

[24] J. Kang, P. Langacker, T.-j. Li and T. Liu, *Electroweak baryogenesis in a supersymmetric* U(1)*-prime model*, Phys. Rev. Lett. **94** (2005) 061801 [hep-ph/0402086] [INSPIRE].

[25] Y. Achiman and B. Stech, *Topless model for grand unification*, in *Advanced Summer Institute on New Phenomena in Lepton and Hadron Physics*, D.E.C. Fries and J. Wess eds., Plenum, New York U.S.A. (1979).

[26] M. Singer, J.W.F. Valle and J. Schechter, *Canonical neutral current predictions from the weak electromagnetic gauge group* $\mathrm{SU}(3) \times \mathrm{U}(1)$, Phys. Rev. **D 22** (1980) 738 [INSPIRE].

[27] F. Pisano and V. Pleitez, *An* $\mathrm{SU}(3) \times \mathrm{U}(1)$ *model for electroweak interactions*, Phys. Rev. **D 46** (1992) 410 [hep-ph/9206242] [INSPIRE].

[28] P.H. Frampton, *Chiral dilepton model and the flavor question*, Phys. Rev. Lett. **69** (1992) 2889 [INSPIRE].

[29] J.C. Montero, F. Pisano and V. Pleitez, *Neutral currents and GIM mechanism in* $\mathrm{SU}(3)L \times \mathrm{U}(1)N$ *models for electroweak interactions*, Phys. Rev. **D 47** (1993) 2918 [hep-ph/9212271] [INSPIRE].

[30] R. Foot, O.F. Hernandez, F. Pisano and V. Pleitez, *Lepton masses in an* $\mathrm{SU}(3)L \times \mathrm{U}(1)N$ *gauge model*, Phys. Rev. **D 47** (1993) 4158 [hep-ph/9207264] [INSPIRE].

[31] J. Maalampi and M. Roos, *Physics of mirror fermions*, Phys. Rept. **186** (1990) 53 [INSPIRE].

[32] J. Erler, P. Langacker, S. Munir and E. Rojas, *Improved constraints on Z-prime bosons from electroweak precision data*, JHEP **08** (2009) 017 [arXiv:0906.2435] [INSPIRE].

[33] F. del Aguila, J. de Blas and M. Pérez-Victoria, *Electroweak limits on general new vector bosons*, JHEP **09** (2010) 033 [arXiv:1005.3998] [INSPIRE].

[34] P. Langacker and M.-x. Luo, *Constraints on additional Z bosons*, Phys. Rev. **D 45** (1992) 278 [INSPIRE].

[35] A. Czarnecki and W.J. Marciano, *Electroweak radiative corrections to polarized Moller scattering asymmetries*, Phys. Rev. **D 53** (1996) 1066 [hep-ph/9507420] [INSPIRE].

[36] J. Erler and M.J. Ramsey-Musolf, *The weak mixing angle at low energies*, Phys. Rev. **D 72** (2005) 073003 [hep-ph/0409169] [INSPIRE].

[37] SLAC E158 collaboration, P.L. Anthony et al., *Precision measurement of the weak mixing angle in Moller scattering*, Phys. Rev. Lett. **95** (2005) 081601 [hep-ex/0504049] [INSPIRE].

[38] Particle Data Group collaboration, K. Nakamura et al., *Review of particle physics*, J. Phys. **G 37** (2010) 075021 [INSPIRE].

[39] Y. Li, F. Petriello and S. Quackenbush, *Reconstructing a Z-prime Lagrangian using the LHC and low-energy data*, Phys. Rev. **D 80** (2009) 055018 [arXiv:0906.4132] [INSPIRE].

[40] W.-F. Chang, J.N. Ng and J.M.S. Wu, *Non-supersymmetric new physics and polarized Moller scattering*, Phys. Rev. **D 79** (2009) 055016 [arXiv:0901.0613] [INSPIRE].

[41] J. Erler, *Global fits to electroweak data using GAPP*, in proceedings of the *Physics at RUN II: QCD and Weak Boson Physics Workshop: 2nd General Meeting*, June 3–4, Batavia, U.S.A. (2000), hep-ph/0005084 [INSPIRE].

[42] K.S. Kumar, *Low energy tests of the standard model: the* 12 *GeV parity violation program at Jefferson Laboratory*, *Int. J. Mod. Phys.* **E 19** (2010) 927 [INSPIRE].

[43] J. Erler, P. Langacker, S. Munir and E. Rojas, *Z' bosons from E_6: collider and electroweak constraints*, arXiv:1108.0685 [INSPIRE].

[44] QWEAK collaboration, W.T.H. van Oers, *The qweak experiment: a search for new physics at the TeV scale*, *Nucl. Phys.* **A 805** (2008) 329 [arXiv:0708.1972] [INSPIRE].

[45] QWEAK collaboration, D. Androic et al., *First determination of the weak charge of the proton*, *Phys. Rev. Lett.* **111** (2013) 141803 [arXiv:1307.5275] [INSPIRE].

[46] J. Erler, C.J. Horowitz, S. Mantry and P.A. Souder, *Weak polarized electron scattering*, *Ann. Rev. Nucl. Part. Sci.* **64** (2014) 269 [arXiv:1401.6199] [INSPIRE].

[47] P. Souder, *Parity-violating DIS at JLab with* 12 *GeV*, *Conf.Proc.* **C0804071** (2008) 243.

[48] K.S. Kumar, S. Mantry, W.J. Marciano and P.A. Souder, *Low energy measurements of the weak mixing angle*, *Ann. Rev. Nucl. Part. Sci.* **63** (2013) 237 [arXiv:1302.6263] [INSPIRE].

[49] J. Erler and S. Su, *The weak neutral current*, *Prog. Part. Nucl. Phys.* **71** (2013) 119 [arXiv:1303.5522] [INSPIRE].

[50] SoLID collaboration, P.A. Souder et al., *Precision measurement of parity-violation in deep inelastic scattering over a broad*, JLab Proposal PR-09-012 (2009).

[51] PVDIS collaboration, D. Wang et al., *Measurement of parity violation in electron-quark scattering*, *Nature* **506** (2014) 67 [INSPIRE].

[52] D. Wang et al., *Measurement of parity-violating asymmetry in electron-deuteron inelastic scattering*, *Phys. Rev.* **C 91** (2015) 045506 [arXiv:1411.3200] [INSPIRE].

[53] C. Wood et al., *Measurement of parity nonconservation and an anapole moment in Cesium*, *Science* **275** (1997) 1759.

[54] J. Erler and M.J. Ramsey-Musolf, *Low energy tests of the weak interaction*, *Prog. Part. Nucl. Phys.* **54** (2005) 351 [hep-ph/0404291] [INSPIRE].

[55] M.R. Buckley and M.J. Ramsey-Musolf, *Precision probes of a leptophobic Z' boson*, *Phys. Lett.* **B 712** (2014) 261 [arXiv:1203.1102] [INSPIRE].

[56] M. González-Alonso and M.J. Ramsey-Musolf, *Leptophobic Z' boson and parity-violating eD scattering*, *Phys. Rev.* **D 87** (2013) 055013 [arXiv:1211.4581] [INSPIRE].